PREPUBLICACIONES DEL DEPARTAMENTO
DE MATEMÁTICA APLICADA
UNIVERSIDAD COMPLUTENSE DE MADRID
MA-UCM 2012-06

Navigation in Time-Evolving Environments Basedon Compact Internal Representation: Experimental Model

José Antonio Villacorta-Atienza and Valeri A. Makarov

Mayo-2012

http://www.mat.ucm.es/deptos/ma
e-mail:matemática_aplicada@mat.ucm.es

Navigation in Time-Evolving Environments Based on Compact Internal Representation: Experimental Model

José Antonio Villacorta-Atienza and Valeri A. Makarov

***Abstract*—Near-range navigation in time-evolving environments requires anticipation of the possible changes in the external world and appropriate adaptation of the agent's behavior. The recently introduced concept of Compact Internal Representation (CIR) efficiently solves both problems simultaneously. CIRs offer static maps for description of essentially time-evolving situations. Here we discuss implementation of the concept in a neural network that enables protocognitive navigation in different dynamic situations observed in the external world. Then we employ this neural network for robot navigation in real time-evolving environments. We show how CIRs can be generated, learned, memorized, and quickly retrieved from the memory for fast decision-making and selection of optimal routes to the target. Experimental results confirm that the CIR-based protocognitive network provides the agent with a reliable, fast, and flexible manner for dealing with dynamic situations.**

I. Introduction

PROTOCOGNITION brings together the primary cognitive abilities required for an intelligent motor interaction with the external world [1]. Even simplest animals can exhibit surprisingly efficient behaviors in complex time-evolving environments (see e.g. [2], [3]). There exists growing experimental evidence that such fascinating abilities are based on effective Internal Representation (IR) of the external world [4]–[7]. The IR makes possible mental simulations, goal planning, testing of alternative behaviors and, as a consequence, an intelligent decision-making [8]. However the mechanisms behind the IR are barely understood both from theoretical and experimental viewpoints [9], [10].

Perception of the environment implies concurrence of diverse sensory modalities that continuously provide complex information about the external world, which must be properly reduced and structured to create useful IR. IR of static situations can be thought about as an abstract "copy" of the external world built from the sensory information obtained at any time-instant. For the purpose of navigation an agent can just project near-range static objects (obstacles and targets) into a mental map and then plan a route to a target. This approach, for example, has been implemented in a neural network with reaction-diffusion dynamics [11]. Then the potential field established in the network under sensory drive is the IR of the given situation.

IR of dynamic situations, i.e. when the environment evolves in time (e.g. objects move in the arena), demands higher level abilities allowing to cope with spatiotemporal information. Generalizing the static approach, one could generate a sequence of static IRs made for each time instant like frames in a movie. This, however, has a number of internal pitfalls: from the obvious increase (virtually infinite) of the memory capacity required for description of the situation, to the ambiguous dynamic treatment of essentially static information. To resolve this problem a number of different approaches has been proposed (for review see [12]): self-organizing neural networks adaptable to dynamic changes in its environment [13], path planning strategies based on changing potential fields [14], recurrent neural networks applied to manipulators [15], and biologically-inspired neural networks for planning obstacle avoidance [16], among others.

Recently, for an efficient description of complex dynamic situations we introduced the so-called concept of Compact Internal Representation (CIR) [17], [18]. The idea behind CIR is based on the modeling of the future and extracting, in a special way, of events critical for the agent (e.g. potential collisions with obstacles), which are then mapped into a static pattern. Thus essentially time-evolving situation is compacted into a static structure, which provides the information necessary to reach the goal. This process takes place in the agent's "mind" and follows two stages implemented in coupled neural networks. The Trajectory Modeling Neural Network (TMNN) predicts the trajectories of the objects in the agent's environment. These trajectories are used by the Causal Neural Network (CNN), which simulates all possible agent's movements according to the predicted evolution of the situation and generates a static mental map (CIR) of collisions with obstacles and targets. By using this map the agent can successfully avoid obstacles in its environment and reach the target.

In this work we discuss implementation of a protocognitive network that permits generation, learning, and fast retrieval of CIRs. We also extend the concept by including mobile targets. Then we present the application of this neural network to robot navigation in real time-evolving environments. We show that CIRs can be learned and memorized for quick decision-making and selection of optimal routes. Thus we show that the CIR-based protocognitive network provides the agent with a reliable, fast, and flexible manner for dealing with dynamic situations.

J.A. Villacorta-Atienza and V.A. Makarov are with the Department of Applied Mathematics, Complutense University of Madrid, Av. Complutense s/n, 28040, Madrid, Spain (http://www.mat.ucm.es/∼vmakarov/).

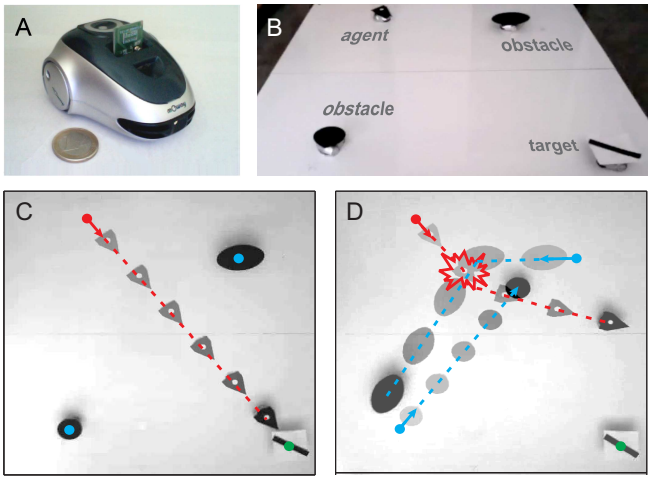

Fig. 1: Experimental setup for robot navigation experiments. A) Roving robot equipped with WiFi interface aside of a 1€ coin. B) 150×150 cm arena with four robots simulating the agent (arrow shape), the obstacles (circular shapes), and the target (stripe). C) Top view of a static situation (captured by a zenithal camera). The agent has a goal to reach the target. Six consecutive frames marking the agent's positions are shown superimposed. D) Dynamic situation. A collision occurs if the agent makes the decision from the initially perceived visual information as in the static case (dots and arrows mark positions and velocities, respectively).

II. Experimental Setup

In order to study the problem of protocognitive near-range navigation we built a setup (Figs. 1A and 1B) with roving robots simulating an agent, one target, and two moving obstacles in a white arena (150×150 cm). The programmable robots (Moway, Minirobots S.L., Fig. 1A) were controlled through a WiFi interface with customary written C# code managed by Matlab (R2010b 64-bit, The MathWorks, Inc.) running on a standard PC. In order to distinguish objects in the arena, black cardboard figures were stuck over each robot (Fig. 1B): arrow-shaped over the agent, circular shapes over the obstacles, and a strip over the target. The visual information in the arena were captured by a zenithal camera (Logitech QuickCam Communicate STX). For object recognition we used the image analysis routines from the Matlab Image Processing Toolbox. The snapshots of the arena were taken at 50 Hz rate. Then all black objects were identified in each frame. The objects were differentiated by the size of black figures stuck over the robots, and the displacement of centroids were used for tracking and for determining positions, velocities, and accelerations of the objects.

Figures 1C and 1D show examples of static and dynamic situations, respectively. Dots with arrows represent initial positions and velocities of the objects in the arena: red for the agent, blue for the obstacles, and green for the target. In the static environment (Fig. 1C) the visual information obtained at the initial moment determines the agent's motor decision. The agent can move along a straight trajectory and easily reach the target. In a similar but dynamic situation both obstacles cross the agent's path (Fig. 1D). The same agent's behavior would lead to a collision. Thus this situation requires from the agent more sophisticated path planning based on the knowledge of the state of the environment in the future. In the following sections we shall show how the CIR concept can be used for this purpose.

III. Trajectory Modeling Neural Network

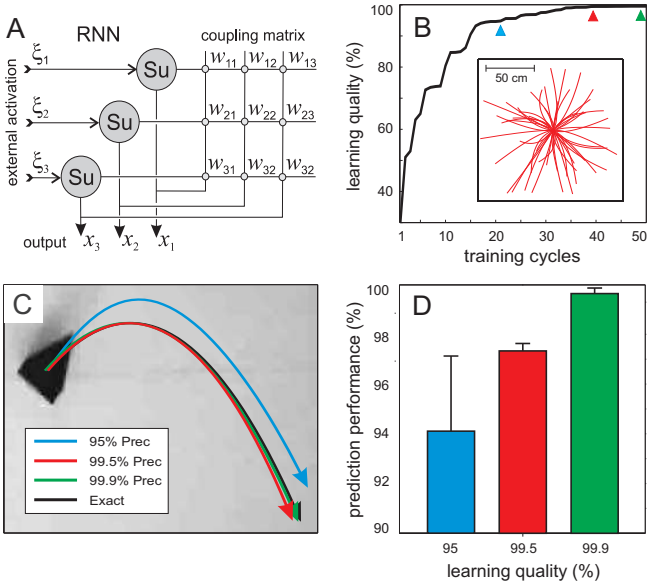

Fig. 2: Prediction of trajectories of moving objects. A) Sketch of a recurrent neural network used for trajectory modeling. B) Learning performance. Blue, red, and green triangles mark the training quality with $d = 95\%$, 99.5%, and 99.9%. Inset shows the trajectories used for training the TMNN. C) Prediction of an experimental trajectory at different levels of the learning quality, corresponding to triangles in (B). D) Mean and standard deviation of the performance of the TMNN in predicting trajectories of 100 objects for three different values of the learning quality.

Generation of a CIR requires prediction (in the agent's mental time τ) of the trajectories of near-range objects in the arena. This task is performed by the Trajectory Modeling Neural Network. Figure 2A shows the implementation of the TMNN. It consists of three recurrently coupled neurons with external inputs $\xi(k) \in \mathbb{R}^3$ and outputs $x(k+1) \in \mathbb{R}^3$, where k denotes discrete mental time (i.e. $\tau = kh$, where h is the time step) [19]. The dynamics of the network is given by

$$x(k+1) = \begin{cases} \xi(k), & \text{if } |\xi(k)| > \delta \\ Wx(k), & \text{otherwise} \end{cases} \quad (1)$$

where $\delta > 0$ is the tolerance constant and $W \in \mathcal{M}_{3\times3}(\mathbb{R})$ is the coupling matrix.

For the sake of simplicity we assume that trajectories of all objects in the environment can be described by quadratic functions of time. In order to train the TMNN to recognize such routes we generated a set of 50 random trajectories (Fig. 2B, inset) and presented them to the network as external input in the form $\xi(k) = (x(k), v(k), a(k))^T$, i.e. the first three dynamic moments of the trajectory. Then the interneuronal couplings are updated according to

$$\begin{aligned} W(k+1) = \; & W(k)\left(I - \varepsilon\xi(k-1)\xi^T(k-1)\right) \\ & +\varepsilon\xi(k)\xi^T(k-1) \end{aligned} \quad (2)$$

where $\varepsilon > 0$ is the learning rate.

Under proper learning rate $\varepsilon < \varepsilon^*$, W converges to a theoretical matrix W_∞ [19]. The distance

$$d(k) = 100\left(1 - \frac{\|W(k) - W_\infty\|}{\|W_\infty\|}\right) \tag{3}$$

is used to quantify the learning performance (Fig. 2B). Indeed, under training the interneuronal couplings quickly converged (in less than 50 cycles) to the theoretically predicted values. For further analysis we selected the coupling matrices W_{95}, $W_{99.5}$, and $W_{99.9}$ corresponding to different learning quality to $d = 95\%$, 99.5%, and 99.9%, respectively.

Once the training process is deemed finished, the TMNN can be used to predict the object's trajectories in the arena. The first three instants of the object's movement are captured and introduced in the TMNN as an internal input consisting of initial position, velocity, and acceleration of the object. Then the TMNN generates the following object's trajectory. Figure 2C shows a top-view of a robot in the arena following the black curve and trajectories produced by the TMNN for three different values of the learning quality.

In order to quantify the TMNN prediction performance we used the Fréchet distance $d_F(c, c^*)$ [22] measuring the similarity between the original robot trajectory c and the trajectory predicted by the TMNN c^*. Then the prediction performance is

$$P(c, c^*) = 100\,(1 - d_F(c, c^*)/l(c)) \tag{4}$$

where $l(c)$ denotes the length of the curve c. Figure 2D shows the statistics of the prediction performance for different values of the learning quality obtained for a set $\{c_i\}_{i=1}^{100}$ of random trajectories. The learning quality achieved in about 50 training cycles is enough to obtain practically 100% fidelity in the prediction of trajectories by the TMNN.

IV. Concept of Compact Internal Representation

Let us briefly recall how a CIR of a dynamic situation can be created and then used for navigation [17], [18]. CIR is generated by a reaction-diffusion process taken place in the CNN, a 60×60 square lattice, described by:

$$\begin{aligned} \dot{r}_{ij} &= q_{ij}\,(H(r_{\rm th} - r_{ij})\,[f(r_{ij}) - v_{ij}] + d\Delta r_{ij} - r_{ij}p_{ij}) \\ \dot{v}_{ij} &= (r_{ij} - 7v_{ij} - 2)/25 \end{aligned} \tag{5}$$

where dots represent derivatives in respect to the mental time τ, Δ is the discrete Laplacian, d is the diffusion constant, $f(r) = (-r^3 + 4r^2 - 2r - 2)/7$, and H is the Heaviside function. Functions $q_{ij}(\tau)$ and $p_{ij}(\tau)$ (equal to one and zero, respectively, at the beginning of the simulation) will be described below.

Let us now consider a dynamic situation similar to that shown in Fig. 1D. The agent (Fig. 3A, blue circle) should move with constant velocity and reach the mobile target (red area) avoiding the moving obstacles (black areas). The initial conditions, i.e. objects' positions, velocities, and accelerations, are supplied to the TMNN that simulates the obstacles and target's trajectories (see Sect. III).

Simultaneously in the CNN a circular wavefront is initiated at the agent's location (Fig. 3B). Propagation of the wavefront in the lattice mentally simulates all possible positions of the agent at each moment in the virtual future. Figures 3B-3G show sequential snapshots of the CNN state. For $\tau = \tau_1$ the first contact of the wavefront and one of the (moving) obstacles occurs (Fig. 3B). This contact marks the place where the agent would collide against the obstacle if the corresponding trajectory were performed in the arena. The cells of the CNN $\{(i^*, j^*)\}$ corresponding to those locations are frozen, i.e. $q_{i^*,j^*}(\tau) = 0$ for $\tau \geq \tau_1$. They constitute an effective obstacle, i.e. a static structure containing the critical spatiotemporal information concerning potential collisions between the agent and the obstacle (Fig. 3D, area filled in black). We note that in general an effective obstacle has a shape different from the shape of the corresponding real obstacle. Therefore the problem of avoidance of moving obstacles in the arena is reduced to the avoidance of static effective obstacles created in the mental map.

In the same fashion interaction between the wavefront and the (mobile and immobile) targets will produce effective targets. Figures 3E-3G show how cells, where the wavefront and the virtual target collide, are frozen by setting $p_{i^*,j^*}(\tau) = 1$ for $\tau \geq \tau_4$ in the network (5) and form an effective target (Fig. 3G, area filled in red). We note that in general one target can create several effective targets, which correspond to different strategies for target catching.

In the region behind the wavefront passive diffusion (controlled by the Heaviside term in (5)) creates a static potential field including the agent position and the effective obstacles and targets. This potential field, i.e. a pattern $\{r_{ij}^*\}$, is the CIR for the considered dynamic situation (Fig. 3H). This field can be used to draw possible trajectories from the initial agent's position to the effective targets by the gradient descend method. Following such trajectories in the arena ensures avoiding obstacles and catching the target.

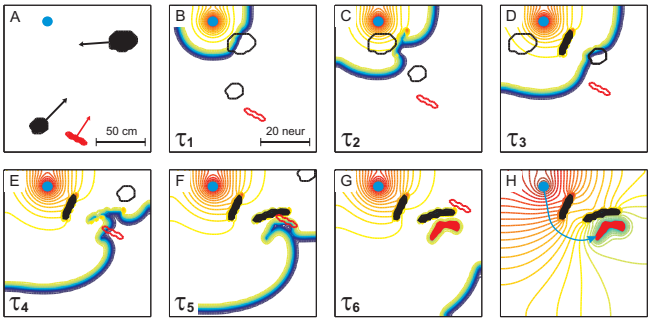

Fig. 3: Generation of Compact Internal Representation of a dynamic situation. A) Initial configuration of the arena. The agent, target, and obstacles are shown in blue, red, and black, respectively, arrows mark their velocities. B)-G) Sequential snapshots of the state of CNN (the pattern $\{r_{ij}(\tau)\}_{i,j=1}^{60}$ is plotted) showing the creation of effective target and obstacles (red and black filled areas, respectively). Virtual positions of the target and obstacles are shown by contour shapes. H) CIR of the considered dynamical situation. The shortest trajectory to the effective target (and thus to the target moving in the arena) is shown by blue curve.

V. Protocognitive Navigation based on CIR

As discussed in the previous section, CIR collapses the time dimension of a dynamic situation by mapping only the critical events (virtual collisions and effective targets) into a static map. Therefore CIR of a dynamic situation is a static pattern (i.e. a matrix $\mathcal{M}_{n\times n}(\mathbb{R})$), which can be learned, stored in memory, retrieved, compared, etc. Thus we can easily manage different realistic experiences in a fast and reliable manner.

Figure 4 shows how such protocognitive abilities can be implemented in a neural network. Protocognition begins with perception of the situation in which the agent is involved. For this purpose in our experimental setup we used visual information from a zenithal perspective of the arena. The perceived situation (a vector $s \in \mathbb{R}^m$ consisting of positions, velocities, and accelerations of all objects) is then supplied to "conscious" and "subconscious" pathways.

The output of both pathways is the CIR (i.e. an $n \times n$ matrix), which contains the required information to solve the navigation problem. The standard gradient descent method provides a trajectory that, transformed in motor orders, permits the agent to reach the target safely (Fig. 4, red curve in the arena). The conscious pathway directly produces CIR for a given sensory vector s. This CIR is also fed back into the subconscious pathway where a recurrent neural network establishes associations between s and the CIR. Then if the agent faces one of the learned experiences it could recover the corresponding CIR in a fast and reliable way. In general subconscious pathway works much faster than the conscious one but requires previous learning. Thus the protocognitive agent requires training for optimal operations in complex environments.

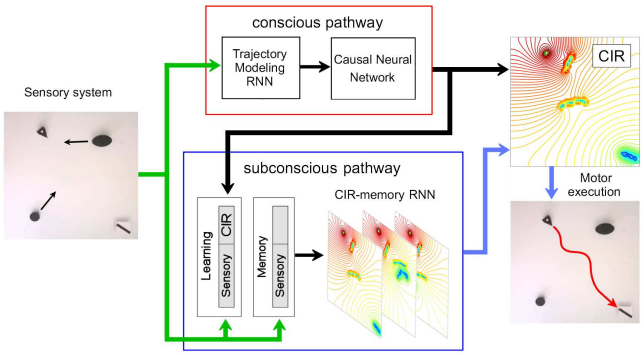

Fig. 4: Block-scheme of CIR-based protocognitive network.

A. Conscious Pathway

The perception of a new situation forces the agent to understand it by "consciously" creating the corresponding CIR (Fig. 4, red box). This process, detailed in Sect. IV, has been implemented for robot navigation.

In order to illustrate the capability of CIR to represent dynamic situations three different time-evolving environments were considered (Figs. 5A-5C). The target is immobile in the simplest situation S_1, whereas in situations S_2 and S_3 it moves in different directions. In all three situations two obstacles cross the agent's path to the target.

Zenithal camera captures 1 s initial interval of the evolution of the robots representing obstacles and target. These initial conditions (sensory vector) are used to mentally simulate the target's and obstacles' trajectories (Sect. III). This information serves as basis for generating the CIR as described in Sect. IV and illustrated in Fig. 3 for S_2.

Figures 5D-5F show the CIRs for S_1, S_2, and S_3, respectively. Note the different shapes and locations of effective targets and obstacles reflecting distinct dynamical circumstances. The obtained CIRs were used to trace a set of suitable trajectories by means of the standard gradient descend method. Blue pathways in Figs. 5D and 5F represent the shortest trajectories solving the corresponding navigation problem for situations S_1 and S_3, respectively. The CIR in Fig. 5E (S_2) admits two trajectories of about the same length. The difference between them is the distinct collision risk to reach the moving target. Nevertheless both trajectories in mental maps shown in Figs. 5D-5F lead the agent to the target with no collisions against obstacles.

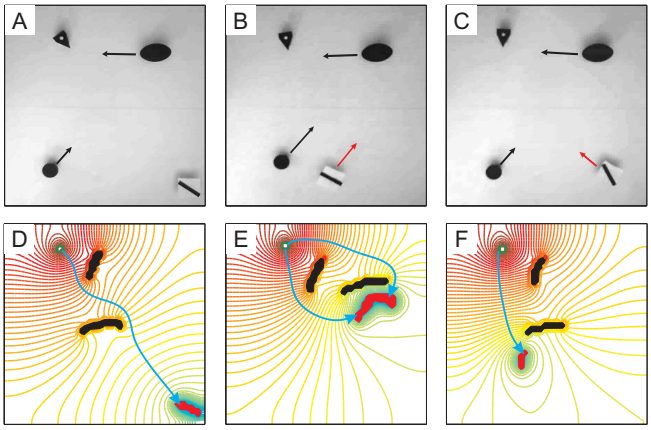

Fig. 5: Navigation based on CIR in three different time-evolving situations S_1, S_2, and S_3. A)-C) Initial configurations for each dynamic situation. Arrows indicate the initial velocities and directions of the objects in the arena. D)-F) The corresponding CIRs created by the "conscious" pathway. Blue curves show trajectories to the effective target.

B. Subconscious Pathway

When the agent faces a familiar, i.e. previously learned, situation the visual information, s, is processed by the subconscious pathway (Fig. 4, blue box). The neural network implementing the subconscious pathway retrieves from the associative memory the CIR corresponding to the sensory information. The general RNN introduced in Sect. III (Fig. 2A) can also learn static patterns [19]–[21]. Since CIRs after all are static patterns linked to specific initial sensory information ($s \in \mathbb{R}^m$) the same RNN but with higher number of neurons can implement a suitable associative memory.

We shall call an experience the union of the initial sensory information about a dynamic situation $s \in \mathbb{R}^m$ and the respective CIR. We ordered each CIR, i.e. a static 2D pattern $\{r^*_{ij}\}^n_{i,j=1}$, into a 1D vector $c \in \mathbb{R}^{n^2}$. Then each experience is a composite vector

$$a = (c, s)^T \in \mathbb{R}^{n^2+m}$$

simultaneously describing the situation and the corresponding CIR. Finally the associative memory is a recurrent neural network shown in Fig. 2A with $(n^2 + m)$ neurons. This network first goes through the learning and then can be used for retrieval of previously learned CIRs.

1) Learning Phase: Learning phase is implemented though sequential presentations to the RNN of a set of p experiences $\{a_i\}_{i=1}^{p}$. At each learning step k the network is exposed to one of the composite vectors a_i and the coupling matrix is updated according to

$$W(k+1) = W(k)\left(I - \varepsilon\xi(k)\xi^T(k)\right) + \varepsilon\xi(k)\xi^T(k) \qquad (6)$$

where $\varepsilon > 0$ is again the learning rate and $\xi(k) \in \{a_i\}_{i=1}^{p}$ is an element from the set of experiences. We note that although the memory RNN and TMNN have the same structure the learning rule (6) differs from (2). Earlier we have shown that this learning process converges [19]. Theoretically the associative memory can store up to $n^2 + m$ experiences.

2) Retrieval Phase: Once the learning phase has been finished the RNN can be used to associate new sensory information s with one of the previously learned experiences $\{a_i\}$ to extract the corresponding CIR c. This is achieved by presenting to the RNN (and maintaining during the retrieval process) the sensory part of one of the learned experiences, say l-th. Then the network activation is given by

$$\xi(k) = (\underbrace{0, 0, \ldots, 0}_{n^2}, s_l)^T \qquad k \geq 0$$

Consequently the last m neurons in the RNN have no dynamics: $x_{n^2+1,\ldots,n^2+m}(k) = s_l,\ k \geq 0$, while the others follow the linear map:

$$y(k+1) = W^* y(k) + B,$$

where $W^* = (w^*_{ij})_{i,j=1}^{n^2}$ is a part of the coupling matrix after learning and $B = \sum_{j=n^2+1}^{n^2+m} w^*_{ij} s_{l;j}$ (here $s_{l;j}$ means the j-th element of the l-th vector). It has been proven that following this scheme the memory completes the missing part of a_l and hence retrieves the stored CIR [18].

C. Numerical Simulations of the Associative Learning

Success of the navigation in dynamic situations depends on the velocity of retrieval and quality of CIRs, and hence on the performance of the associative memory.

To simulate the process of learning and retrieval we used the three dynamic situations S_1, S_2, and S_3 shown in Figs. 5A-5C and the corresponding CIRs (Figs. 5D-5F) generated by the conscious pathway. Then we composed the experience vectors a_1, a_2, and a_3 and presented them several times in arbitriry order to the agent for learning, i.e. for making associations in the RNN modeling the memory (Fig. 4). After learning we examined how the agent solves the navigation problem by presenting each one of the three dynamic situations and studying the retrieved CIRs.

Figure 6 illustrates the results of CIR retrieval for each dynamic situation (columns) after 2, 6, 70, and 220 training cycles (rows). Having passed only two learning cycles is insufficient for navigation, no trajectory to the target can be traced. CIRs retrieved after 6 training cycles reveal mixtures of the original CIRs and also cannot be used for tracing correct trajectories to the target. Thus at the beginning of the training the agent tends to mess different experiences and as a consequence it cannot successfully solve the navigation problem. Keeping training, the quality of CIRs is refined (Fig. 6, $N_{tr} = 70$ cycles) and after 220 training cycles the CIRs retrieved from the memory are practically identical to the original CIRs (compare Fig. 6, bottom row vs Figs. 5D-5F). Thus the memorization of different experiences converges quite rapidly and the subconscious pathway can finally provide real benefit. Indeed, the "conscious" processing of a dynamic situation in a standard PC lasts around 250 s, while the subconscious pathway provides the same CIR in less than 4.5 s. These numbers can be significantly reduced by using parallel multicore calculations or hardware implementation [23], however their ratio (50 folds) will keep constant.

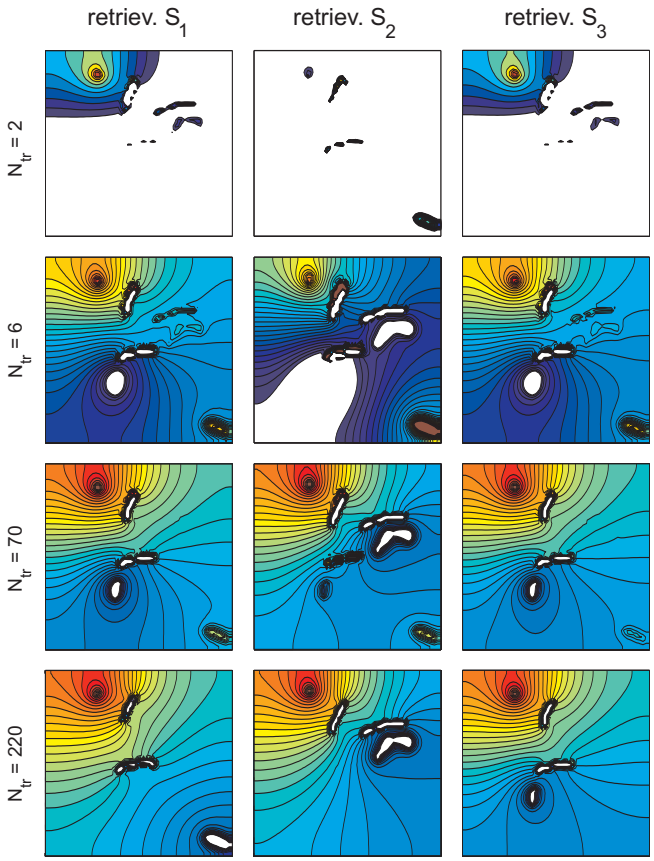

Fig. 6: Associative learning of experiences. Each experience, i.e. the sensory information $s_{1,2,3}$ and the CIRs $c_{1,2,3}$ corresponding to the dynamic situations $S_{1,2,3}$ (Fig. 5), has been learned and then retrieved from the memory. Rows correspond to retrieval after $N_{tr} = 2$, 6, 70 and 220 learning cycles.

D. Experimental Verification of Protocognitive Navigation

Let us now present experimental results for the situations shown in Figs. 5A-5C. Once the sensory information of a specific situation has been processed and the corresponding CIR

has been obtained (either by the conscious or by the subconscious pathway), the obtained trajectories are transformed into motor commands for the agent. Then all robots simulating the agent, the target, and obstacles (Fig. 1B) are simultaneously activated. For each situation the zenithal camera captures the trajectory executed by the agent to compare it with the pathway obtained from the CIR (Figs. 5D-5F).

1) Conscious Pathway: Figures 7A-7C show navigation in the dynamic situations S_1, S_2, and S_3, respectively. In all situations the agent successfully caught the target and avoided obstacles[1]. The reliability of this experimental procedure is quantified by comparing theoretical $\{T_i\}_{i=1}^4$ and experimental $\{C_i\}_{i=1}^4$ trajectories using the measure (4). We obtained $\langle P(T_i, C_i)\rangle = 2.6\%$ with standard deviation 0.18%.

Figures 7D shows statistical data for twelve experiments. We quantified the minimal experimental distance from the agent to the obstacles related to the agent's size. This measure describes the safeness of the agent's movements. In average the agent passes no closer than 1.5 agent's size to the obstacles, which is sufficient for most applications. The achievement of the goal is quantified by the minimum distance between the agent and the target. Note that the theoretical distance in this case is equal to zero by construction. The most important source of experimental variability in this measure is the error in robots' initial positions, orientations, and velocities in each navigation experiment. Nevertheless we observe high level of success of protocognitive navigation. The average agent proximity to the target is below 30% of the robot's size, which is again acceptable for most of applications.

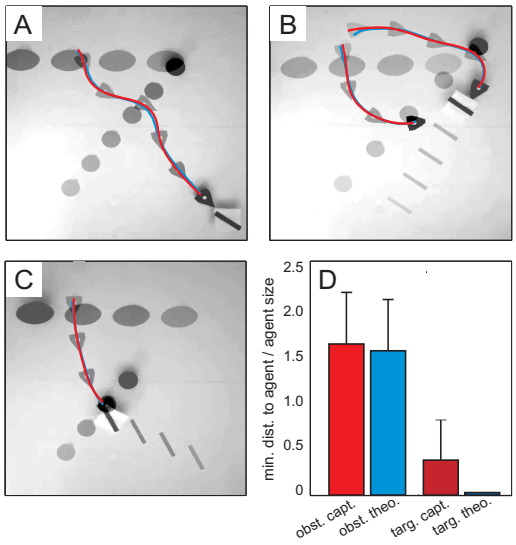

Fig. 7: Robot navigation in dynamic situations based on CIR. A)-C) Superimposed sequence of snapshots (last frame is shown darker) for situations shown in Fig. 5. Blue curves show theoretical trajectories and red curves mark the robot pathways. D) Statistical measures of the navigation performance. Left bars represent means and standard deviations for the minimal distance between the agent and the obstacles (trajectory safeness). Right bars correspond to the final distance to the target (goal achievement). The distance is given in relative units in respect to the agent's size.

[1]Videos with robot experiments and numerical simulations can be found at http://www.mat.ucm.es/∼vmakarov/research.php.

2) Subconscious Pathway: The subconscious processing requires a proper learning of the experiences. Figure 8A shows the CIR for the situation S_1 retrieved from the memory after 6 training cycles. Above we showed (Fig. 6) that the CIR obtained at earlier stages of the learning provides fake effective obstacles and targets. Indeed two trajectories obtained from this CIR (Fig. 8A, blue lines) lead the agent to such a fictitious target, i.e. the agent fails to catch the target. Figure 8B shows experimental trajectories performed by the robot in these conditions. In both cases the robot avoids the obstacles presented in the arena, however, it does not reach the target staying in the right bottom corner. In accordance with our numerical results, at advanced learning stages (i.e. after 200 training cycles) the robot retrieves from the memory high quality CIR and hence follows correct trajectory leading to the target (Fig. 8C).

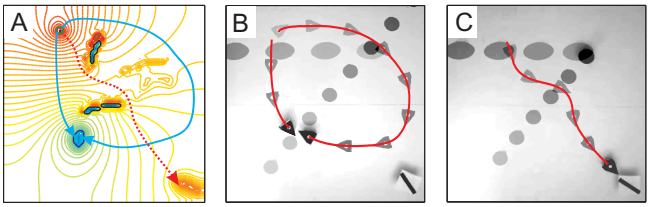

Fig. 8: Robot navigation using subconscious pathway. A) CIR corresponding to the situation S_1 (Fig. 5) retrieved from memory after 6 training cycles. The obtained trajectories (blue curves) go to the fake target, i.e. the agent does not catch the target. Red curve shows the correct trajectory corresponding to a CIR retrieved after 200 training cycles. B) Two trajectories (red curves) performed by the robot to the fake target after 6 training cycles. C) The robot trajectory catching the target after 200 training cycles.

VI. Discussion

Near-range navigation in time-evolving environments requires anticipation of possible changes in the external world and appropriate adaptation of the agent's behavior. In this paper we theoretically developed and experimentally verified the concept of Compact Internal Representation that offers efficient solution to the navigation problem. We have shown that CIR-based neural network consisting of "conscious" and "subconscious" pathways provides the agent with protocognitive abilities and allows reliable and flexible navigation in realistic time-evolving environments.

CIRs are static mental maps containing critical spatiotemporal information about both static and dynamic environments. Avoiding effective obstacles and catching effective targets in such a map ensure avoidance of real obstacles and reaching real targets in the arena. Thus CIRs provides simple (static) but flexible solutions for the navigation problem in time-evolving environments. We have extended the earlier proposed CIR concept by including mobile targets.

When the agent is involved in a situation never experienced before the conscious pathway made of two coupled Trajectory Modeling and Causal Neural Networks generates the CIR of the situation. We have shown that TMNN can quickly learn (in less than 50 training cycles in our experiments) different trajectories and then reliably predict them. In turn the CNN

indeed guarantees that the obtained CIRs allow the agent to avoid obstacles and catch the target. In experiments with a robot platform we obtained the mean shortest distance to the obstacles and to the target about 150% and 30% of the agent's size, respectively. These values are acceptable for most applications.

We notice that our experimental setup reproduces the essence of prototypic situations observed in the nature: animals capture preys and avoid predators. Then survival in quickly changing external world critically depends on fast decision-making. To fulfill this requirement we included the subconscious pathway that allows learning experiences and storing them in associative memory. The latter is facilitated by the fact that CIRs are static 2D patterns, i.e. constant matrices or vectors. We described a Recurrent Neural Network that implements the associative memory and we have shown that such memory can effectively store the agent's experiences (i.e., sensory information and the corresponding CIR). In experiments about 200 training cycles were necessary to learn three similar but different dynamic situations. Then if the agent faces a previously learned situation, the perception of the familiar experience triggers the subconscious fast recovery of the learned CIR. We have shown that a robot supplied with the subconscious pathway can quickly retrieve CIRs and generate trajectories avoiding moving obstacles and reaching mobile targets. Thus the constructed protocognitive agent, with acquired experience, is able to navigate in complex situations adapting itself even to non-predictable changes in the environment.

ACKNOWLEDGMENT

This work has been supported by the Spanish Ministry of Science and Innovation under grant FIS2010-20054.

REFERENCES

[1] R. Wray, C. Lebiere, P. Weinstein, K. Jha, J. Springer, T. Belding, B. Best, and V. Parunak, "Towards a Complete, Multi-level Cognitive Architecture". *Proceedings of the International Conference for Cognitive Modeling*, 27-29, 2007.

[2] B. Milner, L. R. Squire, and E. R. Kandel, "Cognitive Neuroscience and the Study of Memory", *Neuron*, Vol. 20, 445-468, 1998,

[3] R. Menzel and U. Müller, "Learning and Memory in Honeybees: from Behavior to Neural Substrates", *Annual review of neuroscience*, Vol. 19, 379-404, 1996.

[4] R. A. P. Roche, M. A. Mangaoang, S. Commins, and S. M. O'Mara, "Hippocampal Contributions to Neurocognitive Mapping in Humans: A New Model", *Hippocampus*, Vol. 15, 622-641, 2005.

[5] J. O'Keefe and J. Dostrovsky, "The hippocampus as a spatial map. Preliminary evidence from unit activity in the freely-moving rat", *Brain Research*, Vol. 34(1), 171-175, 1971.

[6] E. L. Moser and M. B. Moser, "A metric for space", *Hippocampus*, Vol. 18(12), 1142-1156, 2008.

[7] J. McIntyre, M. Zago, A. Bertho, and F. Lacquaniti, "Does the brain model Newtons laws?", *Nature Neuroscience*, Vol. 4, 693-694, 2001.

[8] T. S. Collett and J. Zeil, "Places and landmarks: an arthropod perspective". In: Healy S (ed) *Spatial representation in animals*. Oxford University Press, Oxford, 18-53, 1998.

[9] E. L. Moser, E. Kropff, and M. B. Moser, "Place cells, grid cells, and the brains spatial representation system", *Annual Review of Neuroscience*, Vol. 31, 69-89, 2008.

[10] T. Hafting, M. Fyhn, S. Molden, M. B. Moser, and E. L. Moser, "Microstructure of a spatial map in the entorhinal cortex", *Nature*, Vol. 436(7052), 801-806, 2005.

[11] G. K. Schmidt and K. Azarm, "Mobile robot navigation in a dynamic world using an unsteady diffusion equation strategy", *Proceedings of International Conference on Intelligent Robots and Systems IEEE/RSJ*, 642-647, 1992.

[12] V. Kunchev, L. Jain, V. Ivancevic, and A. Finn, "Path Planning and Obstacle Avoidance for Autonomous Mobile Robots: A Review", *Lecture Notes in Computer Science*, Vol. 4252/2006, 537-544, 2006.

[13] R. Araújo, "Prune-Able Fuzzy ART Neural Architecture for Robot Map Learning and Navigation in Dynamic Environments", *IEEE Transactions on Neural Networks*, Vol. 17(5), 1235-1249, 2006.

[14] F. Arambula and M. A. Padilla, "Autonomous Robot Navigation using Adaptive Potential Fields", *Mathematical and Computer Modelling*, Vol. 40, 1141-1156, 2005.

[15] U. Steinkühler and H. Cruse, "A holistic model for an internal representation to control the movement of a manipulator with redundant degrees of freedom", *Biological Cybernetics*, Vol. 79, 457-466, 1998.

[16] S. X. Yang and M. Q.-H. Meng, "Real-Time Collision-Free Motion Planning of a Mobile Robot Using a Neural Dynamics-Based Approach", *IEEE Transactions on Neural Networks*, Vol 14(6), 1541-1552, 2003.

[17] J. A. Villacorta-Atienza, M. G. Velarde, and V. A. Makarov, "Compact internal representation of dynamic situations: Neural network implementing the causality principle", *Biological Cybernetics*, Vol. 103, 285-297, 2010.

[18] V. A. Makarov and J. A. Villacorta-Atienza, "Compact internal representation as a functional basis for protocognitive exploration of dynamic environments", *Recurrent Neural Networks for Temporal Data Processing*. Ed. InTech. 81102, 2011.

[19] V. A. Makarov, Y. Song, M. G. Velarde, D. Hubner, and H. Cruse, "Elements for a general memory structure: properties of recurrent neural networks used to form situation models", *Biological Cybernetics*, Vol. 98, 371-395, 2008.

[20] S. Kühn, W. J. Beyn, and H. Crus, "Modelling memory functions with recurrent neural networks consisting of input compensation units: I. Static situations", *Biological Cybernetics*, Vol. 96, 455-470, 2007.

[21] S. Kühn, W. J. Beyn, and H. Crus, "Modelling memory functions with recurrent neural networks consisting of input compensation units: II. Dynamic situations", *Biological Cybernetics*, Vol. 96, 471-486, 2007.

[22] T. Eiter and H. Mannila, "Computing discrete Fréchet distance", *Tech. Report CD-TR 94/64*, Christian Doppler Laboratory for Expert Systems, TU Vienna, Austria, 1994.

[23] L. Salas, L. Alba, and J. A. Villacorta-Atienza. "FPGA implementation of a modified FitzHugh-Nagumo neuron-based causal neural network for compact internal representation of dynamic environments", *Proceedings in SPIE Microtechnologies in Bioelectronics, Biomedical, and Bio-inspired Systems*, 80680J - 9, 2011.

PREPUBLICACIONES DEL DEPARTAMENTO
DE MATEMÁTICA APLICADA
UNIVERSIDAD COMPLUTENSE DE MADRID
MA-UCM 2011

1. APPROXIMATING TRAVELLING WAVES BY EQUILIBRIA OF NON LOCAL EQUATIONS, J. M. Arrieta, M. López-Fernández and E. Zuazua.

2. INFINITELY MANY STABILITY SWITCHES IN A PROBLEM WITH SUBLINEAR OSCILLATORY BOUNDARY CONDITIONS, A. Castro and R. Pardo

3. THIN DOMAINS WITH EXTREMELY HIGH OSCILLATORY BOUNDARIES, J́. M. Arrieta and M. C. Pereira

4. FROM NEWTON EQUATION TO FRACTIONAL DIFFUSION AND WAVE EQUATIONS, L. Váquez

5. EL CÁLCULO FRACCIONARIO COMO INSTRUMENTO DE MODELIZACIÓN, L. Váquez and M. P. Velasco

6. THE TANGENTIAL VARIATION OF A LOCALIZED FLUX-TYPE EIGENVALUE PROBLEM, R. Pardo, A. L. Pereira and J. C. Sabina de Lis

7. IDENTIFICATION OF A HEAT TRANSFER COEFFICIENT DEPENDING ON PRESSURE AND TEMPERATURE, A. Fraguela, J. A. Infante, Á. M. Ramos and J. M. Rey

8. A NOTE ON THE LIOUVILLE METHOD APPLIED TO ELLIPTIC EVENTUALLY DEGENERATE FULLY NONLINEAR EQUATIONS GOVERNED BY THE PUCCI OPERATORS AND THE KELLER–OSSERMAN CONDITION, G. Díaz

9. RESONANT SOLUTIONS AND TURNING POINTS IN AN ELLIPTIC PROBLEM WITH OSCILLATORY BOUNDARY CONDITIONS, A. Castro and R. Pardo

10. BE-FAST: A SPATIAL MODEL FOR STUDYING CLASSICAL SWINE FEVER VIRUS SPREAD BETWEEN AND WITHIN FARMS. DESCRIPTION AND VALIDATION. B. Ivorra B. Martínez-López, A. M. Ramos and J.M. Sánchez-Vizcaíno.

11. FRACTIONAL HEAT EQUATION AND THE SECOND LAW OF THERMODYNAMICS, L. Vázquez , J. J. Trujillo and M. P. Velasco

12. LINEAR AND SEMILINEAR HIGHER ORDER PARABOLIC EQUATIONS IN R^N, J. Cholewa and A. Rodríguez Bernal

13. DISSIPATIVE MECHANISM OF A SEMILINEAR HIGHER ORDER PARABOLIC EQUATION IN R^N, J. Cholewa and A. Rodríguez Bernal

14. DYNAMIC BOUNDARY CONDITIONS AS A SINGULAR LIMIT OF PARABOLIC PROBLEMS WITH TERMS CONCENTRATING AT THE BOUNDARY, A. Jiménez-Casas and A. Rodríguez Bernal

15. DISEÑO DE UN MODELO ECONÓMICO Y DE PLANES DE CONTROL PARA UNA EPIDEMIA DE PESTE PORCINA CLÁSICA, E. Fernández Carrión, B. Ivorra, A. M. Ramos, B. Martínez-López, Sánchez-Vizcaíno.

16. BIOREACTOR SHAPE OPTIMIZATION. MODELING, SIMULATION, AND SHAPE OPTIMIZATION OF A SIMPLE BIOREACTOR FOR WATER TREATMENT, J. M. Bello Rivas, B. Ivorra, A. M. Ramos, J. Harmand and A. Rapaport

17. THE PROBABILISTIC BROSAMLER FORMULA FOR SOME NONLINEAR NEUMANN BOUNDARY VALUE PROBLEMS GOVERNED BY ELLIPTIC POSSIBLY DEGENERATE OPERATORS, G. Díaz

PREPUBLICACIONES DEL DEPARTAMENTO
DE MATEMÁTICA APLICADA
UNIVERSIDAD COMPLUTENSE DE MADRID
MA-UCM 2012

1. ON THE CAHN-HILLIARD EQUATION IN H^1(R^N), J. Cholewa and A. Rodríguez Bernal

2. GENERALIZED ENTHALPY MODEL OF A HIGH PRESSURE SHIFT FREEZING PROCESS, N. A. S. Smith, S. S. L. Peppin and A. M. Ramos

3. 2D AND 3D MODELING AND OPTIMIZATION FOR THE DESIGN OF A FAST HYDRODYNAMIC FOCUSING MICROFLUIDIC MIXER, B. Ivorra, J. L. Redondo, J. G. Santiago, P.M. Ortigosa and A. M. Ramos

4. SMOOTHING AND PERTURBATION FOR SOME FOURTH ORDER LINEAR PARABOLIC EQUATIONS IN R^N, C. Quesada and A. Rodríguez-Bernal

5. NONLINEAR BALANCE AND ASYMPTOTIC BEHAVIOR OF SUPERCRITICAL REACTION-DIFFUSION EQUATIONS WITH NONLINEAR BOUNDARY CONDITIONS, A. Rodríguez-Bernal and A. Vidal-López

6. NAVIGATION IN TIME-EVOLVING ENVIRONMENTS BASED ON COMPACT INTERNAL REPRESENTATION: EXPERIMENTAL MODEL, J. A. Villacorta-Atienza and V.A. Makarov